

# The 2015 superoutburst of QZ Virginis: Detection of growing superhumps between the precursor and main superoutburst

**Akira IMADA<sup>1</sup>, Taichi KATO<sup>2</sup>, Keisuke ISOGAI<sup>2</sup>, Franz-Josef HAMBSCH<sup>345</sup>,  
Pavol A. DUBOVSKY<sup>6</sup>, Igor KUDZEJ<sup>6</sup>, Roger D. PICKARD<sup>7</sup>, Hidehiko  
AKAZAWA<sup>8</sup>, Kiyoshi KASAI<sup>9</sup>, Hiroshi ITOH<sup>10</sup>, Lewis M. COOK<sup>11</sup> and  
Seiichiro KIYOTA<sup>12</sup>**

<sup>1</sup>Kwasan and Hida Observatories, Kyoto University, Yamashina, Kyoto 607-8471, Japan

<sup>2</sup>Department of Astronomy, Faculty of Science, Kyoto University, Sakyo-ku, Kyoto 606-8502, Japan

<sup>3</sup>Groupe Européen d'Observations Stellaires (GEOS), 23 Parc de Levesville, 28300 Bailleau l'Evêque, France

<sup>4</sup>Bundesdeutsche Arbeitsgemeinschaft für Veränderliche Sterne (BAV), Munsterdamm 90, 12169 Berlin, Germany

<sup>5</sup>Vereniging Voor Sterrenkunde (VVS), Oude Bleken 12, 2400 Mol, Belgium

<sup>6</sup>Vihorlat Observatory, Mierova 4, 06601 Humenne, Slovakia

<sup>7</sup>The British Astronomical Association, Variable Star Section (BAA VSS), Burlington House, Piccadilly, London, W1J 0DU, UK; 3 The Birches, Shobdon, Leominster, Herefordshire, HR6 9NG, UK

<sup>8</sup>Department of Biosphere-Geosphere System Science, Faculty of Informatics, Okayama University of Science, 1-1 Ridai-cho, Okayama, Okayama 700-0005, Japan

<sup>9</sup>Baselstrasse 133D, CH-4132 Muttenz, Switzerland

<sup>10</sup>Variable Star Observers League in Japan (VSOLJ), 1001-105 Nishiterakata, Hachioji, Tokyo 192-0153, Japan

<sup>11</sup>Center for Backyard Astrophysics Concord, 1730 Helix Ct. Concord, CA 94518, USA

<sup>12</sup>VSOLJ, 7-1 Kitahatsutomi, Kamagaya, Chiba 273-0126, Japan

\*E-mail: a\_imada@kwasan.kyoto-u.ac.jp

Received 2017 January 27; Accepted 2017 June 5

## Abstract

We report on time-resolved photometry of the 2015 February–March superoutburst of QZ Virginis. The superoutburst consisted of a separated precursor, main superoutburst, and re-brightening. We detected superhumps with a period of  $0.061181(42)$  d between the precursor and main superoutburst. Based on analyses of period changes and amplitudes of superhumps, the observed superhumps were identified as growing superhumps (stage A superhumps). The duration of stage A superhumps was about 5 d, unusually long for SU UMa-type dwarf novae. Using the obtained stage A superhump period, we estimated the mass ratio of QZ Vir to be  $0.108(3)$ . This value suggests that QZ Vir is an SU UMa-type dwarf nova evolving toward the period minimum. Based on the present and the previous observations regarding long-lasting stage A superhumps, a time scale of stage A superhumps is likely to be determined by the mass ratio of the system and the temperature of the accretion disk.

**Key words:** accretion, accretion disks — stars: dwarf novae — stars: individual (QZ Virginis) — stars: novae, cataclysmic variables — stars: oscillations

## 1 Introduction

Cataclysmic variables are close binary systems that consist of a primary white dwarf and a secondary star. The secondary star fills its Roche lobe, transferring mass into the primary Roche lobe. If the magnetic field of the white dwarf is weak ( $< 10$  MG), an accretion disk is formed around the white dwarf (for a review, see Warner 1995; Hellier 2001).

Dwarf novae are a subclass of cataclysmic variables (for a review, see Osaki 1996). A long-term light curve of dwarf novae is well reproduced by the disk instability model (Osaki 1974). When the surface density of the accretion disk reaches the high critical point, an instability within the accretion disk sets in and a large amount of the gas fall onto the white dwarf. This is observed as an outburst. On the other hand, when the surface density reaches the low critical point during the outburst, the gas accretion ceases. This is observed as the end of the outburst. The physical mechanism for the disk instability model is well explained by the thermal limit cycle instability (thermal instability) of ionized and neutral hydrogen (Meyer, Meyer-Hofmeister 1981; Cannizzo 1993; Lasota 2001).

SU UMa-type dwarf novae, one subclass of dwarf novae, have two types of outbursts. One is the normal outburst, whose duration is a few days. The other is the superoutburst, whose duration is as long as 10 days and the maximum magnitude is brighter than that of the normal outburst. The light curve of the normal outburst is reproduced by the thermal instability model. On the other hand, the light curve of the superoutburst is reproduced by the combination of the thermal and tidal instability model (Osaki 1989).<sup>1</sup> When the disk radius reaches the 3:1 resonance between the Keplerian motion of the disk and the orbital motion of the secondary, the gas at the 3:1 resonance radius deviates from the circular orbit, which propagates into the entire disk. As a result, the accretion disk is deformed to a non-axisymmetric structure, which causes a significantly enhanced tidal dissipation and torque on

the accretion disk (Whitehurst 1988; Hirose, Osaki 1990). This results in a long-lasting outburst (superoutburst). During the superoutburst, tooth-like modulations with amplitudes of  $\sim 0.2$  mag, termed superhumps, are observed. The superhump period is slightly longer (typically 1~3 % longer) than the orbital period of the system. This is understood as prograde precession of a tidally-deformed eccentric accretion disk (Osaki 1989).

One of the most important studies concerning photometry of superoutbursts is to examine how the superhump period changes during the course of the superoutburst. Extensive statistical surveys for the superhump period changes have been performed by T. Kato and his colleagues (Kato et al. 2009; Kato et al. 2010; Kato et al. 2012; Kato et al. 2013; Kato et al. 2014b; Kato et al. 2014a; Kato et al. 2015; Kato et al. 2016b). They have established a "textbook" of superhump period changes, which consist of three stages: a long and constant period (stage A), increasing period (stage B), and short and constant period (stage C) (see also figure 3 of Kato et al. (2009)). Although the working mechanisms causing superhump period changes are still unclear, our understanding on stage A superhumps has been significantly improved over the past few years.

Osaki, Kato (2013b) studied Kepler light curves of SU UMa-type dwarf novae V344 Lyr and V1504 Cyg. They suggest that superhump period changes are caused by dynamical precession, pressure effect, or wave-wave interaction of the accretion disk. Osaki, Kato (2013b) further noted that pressure effect and wave-wave interaction are negligible at the onset of appearance of superhumps. This means that the period of stage A superhumps corresponds to the dynamical precession rate of the accretion disk at the 3:1 resonance radius. This interpretation is supported by Kato, Osaki (2013), in which they studied eclipsing dwarf novae and showed that the mass ratios derived by stage A superhump periods are in good agreement with those derived by eclipses. At present, measuring stage A superhump period has become one of the most powerful tools for estimating the mass ratio of the system (Kato et al. 2014c; Ohshima et al. 2014; Isogai et al. 2016).

Statistical studies have revealed that the system showing a long duration of stage A superhumps tends to have a small mass ratio (Kato 2015). This trend is particular-

<sup>1</sup> On the other hand, there are two models in order to explain the superoutburst: the enhanced mass transfer model in which the superoutburst is caused by the enhanced mass transfer from the secondary (e.g., Smak 1991; Schreiber et al. 2004), and the pure thermal limit cycle model in which the superoutburst is explained by the thermal limit cycle model (e.g., Cannizzo et al. 2010; Cannizzo et al. 2012). See Osaki, Kato (2013a) for a review.

ily seen in WZ Sge-type dwarf novae (for a review of WZ Sge-type dwarf novae, see Kato 2015). In recent years, observations showed that stage A superhumps lasted for  $\sim 5$  d in a faint stage between the precursor and the main superoutburst of a newly confirmed SU UMa-type dwarf novae PM J03338+3320 (Kato et al. 2016a). Although the duration of stage A superhumps in PM J03338+3320 was comparable to that of WZ Sge-type dwarf novae, the mass ratio was estimated to be 0.17, an average value for SU UMa-type dwarf novae (Kato et al. 2016a). At present, although it is a very rare event, two SU UMa-type dwarf novae showed long-lasting stage A superhumps in a faint stage between the precursor and the main superoutburst: PM J03338+3320 and V1504 Cyg (Kato et al. 2016a; Osaki, Kato 2014).

QZ Vir (originally named as T Leo) is one of the most notable dwarf novae. The observational history of the object dates back to the 1860s (Peters 1865). Spectroscopic observations revealed the short orbital period of  $84.69936(68)$  min ( $= 0.058819(1)$  d) (Shafter, Szkody 1984). The SU UMa nature of the object was confirmed by Slovak et al. (1987) and Kato, Fujino (1987) during the 1987 January superoutburst after detection of superhumps. However, the lack of observations prevented an accurate determination of the superhump period. Lemm et al. (1993) performed photometry of QZ Vir during the 1993 January superoutburst, during which they obtained the mean superhump period of  $86.7 \pm 0.1$  min ( $0.060208(69)$  d). This period was also confirmed by Kato (1997) in the same superoutburst. On the other hand, some authors have pointed out unusual properties of QZ Vir. For example, Vrielmann et al. (2004) detected a signal at 414 s in X-ray light curves, which they interpreted as the spin period of the white dwarf, or quasi-periodic oscillations. Shafter, Szkody (1984) pointed out a possibility of unusually large mass ratio of the system ( $q \sim 0.48$ , see also figure 11 of Shafter, Szkody 1984), based on their spectroscopic and photometric observations during quiescence. These arguments have obscured an evolutionary status of QZ Vir.

On 2015 February 21.512 (JD 2457075.012), Rod Stubbings reported that QZ Vir was at a visual magnitude of 15.0, about 1 mag brighter than quiescence. After that, QZ Vir brightened to 13.3 on February 21.692 ([vsnet-alert 18318]). On 2015 February 22.919, a visual magnitude reached 10.6, then the system faded again ([vsnet-alert 18334]). On 2015 March 4.885 (JD 2457086.385), QZ Vir rebrightened at a visual magnitude of 10.5 ([vsnet-alert 18371]). It turned out that the latter outburst was indeed a superoutburst which was accompanied by a separate precursor, similar to that observed in PM J03338+3320 and

V1504 Cyg. Thanks to the early discovery of the outburst, we succeeded in detecting growing superhumps (stage A superhumps) of QZ Vir from the end of the precursor in unprecedented detail. The present observations enables us to determine the evolutionary status of the system for the first time, and improves our understanding of stage A superhumps. In section 2, we present our observations. In section 3, we show the main results of the superoutburst. Discussion is given in section 4. We summarize our studies in section 5.

## 2 Observations

Time-resolved CCD photometry was performed between 2015 Feb. 26 and 2015 Mar. 30 (JD 2457080.4585–7111.8066) at 8 sites using 20–40 cm reflecting telescopes. The log of observations is listed in table 1. Although some of the data were acquired with *V* and *R* band filters, the most of the data were acquired without filters. The total datapoints amount to 4689, sufficient to study superhump period changes. Exposure times were 30–180 seconds, with read-out times typically an order of seconds.

After debiasing and flat-fielding, the images were processed with aperture photometry (see table 1). The data obtained were adjusted to the HaC system, in which the star located at RA:11:37:55.92 Dec:03:23:13.5 (*V* = 13.247, *R* = 12.847) was used as the comparison star. The constancy of the comparison star was checked mainly by the star located at RA:11:38:30.54 Dec:03:25:53.3 (*V* = 14.396, *R* = 13.970) and nearby stars in the same image. The times of all observations were converted to Barycentric Julian Date (BJD).

## 3 Results

### 3.1 Overall light curve

Figure 1 shows the overall light curve of the present outburst. As can be seen in this figure, the light curve consists of three outbursts. Although the initial outburst is separated from the subsequent superoutburst, this outburst can be regarded as a precursor, since superhumps were detected after the end of the precursor (see also the next subsection). The duration of the faint stage between the precursor and the main superoutburst was  $\sim 5$  d. We caught the rising stage of the superoutburst on BJD 2457085, when QZ Vir brightened at a rate of steeper than  $-3.3$  mag/d. This value was typical for SU UMa-type dwarf novae (Otulakowska-Hypka et al. 2016). Although our observations were absent between BJD 2457086–88, the brightness maximum may have occurred around BJD

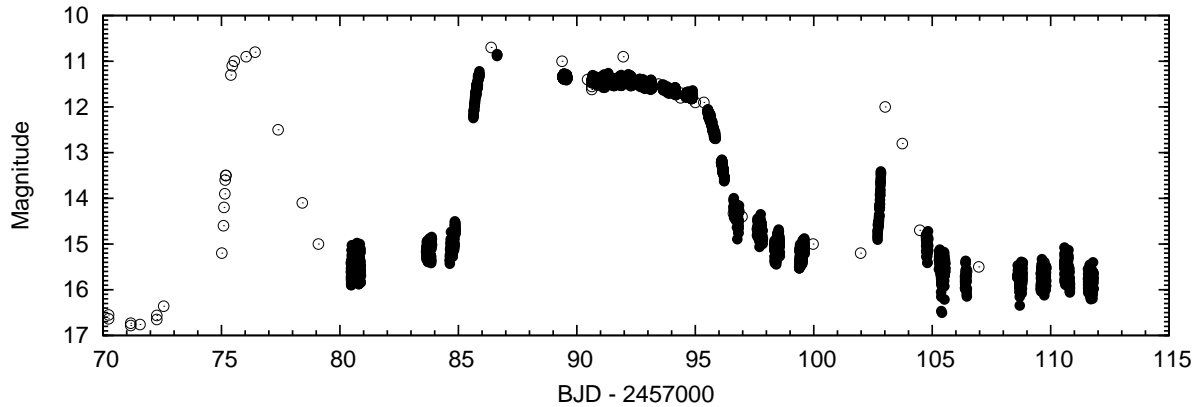


**Fig. 1.** Overall light curve during the 2015 superoutburst. Black points indicate CCD observations, while white points indicate visual observations posted to the AAVSO. Note that the main superoutburst is accompanied by a separated precursor and rebrightening.

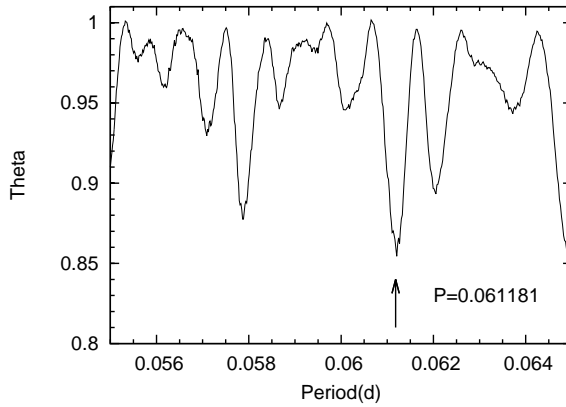


**Fig. 2.** PDM analysis between BJD 2457080.64–85.88. The strongest signal corresponds to  $0.061181(42)$  d, 4.0 % longer than the orbital period of QZ Vir.

2457086. The magnitude kept almost constant at  $\sim 11.5$  mag between BJD 2457089–91, after which the magnitude linearly faded at a rate of 0.13 mag/d. The duration of the plateau stage was  $\sim 9$  d. On BJD 2457095, QZ Vir entered a rapid fading stage, during which the magnitude faded at a rate of 1.9 mag/d. After the end of the main superoutburst, the magnitude slowly faded at a rate of 0.2 mag/d. A rebrightening was observed on BJD 2457103. The light curve of the rebrightening was typical for that observed in SU UMa-type dwarf novae (see, e.g., figure 55 of Kato et al. 2012, figure 16 of Kato et al. 2014b).

### 3.2 Superhumps

One of the noticeable results was that superhumps appeared from the end of the precursor. On BJD 2457080, when the magnitude returned to the quiescent level, superhumps were visible with an amplitude of  $\sim 0.8$  mag. On BJD 2457083–84, the light curve still sustained super-

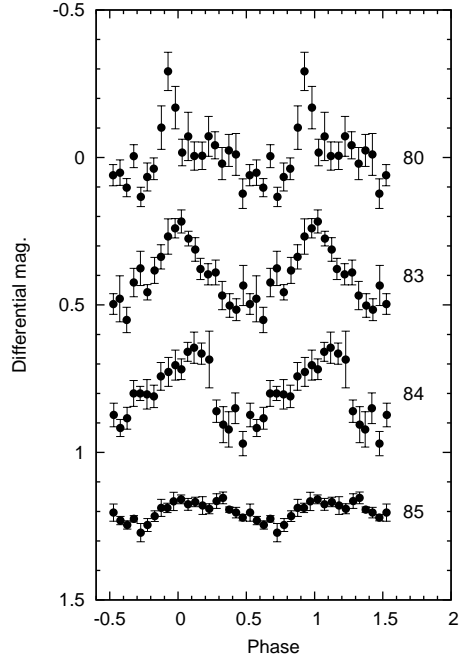


**Fig. 3.** Phase-averaged light curves folded with  $0.061181$  d. The numbers in this figure denote the day since BJD 2457000.

humps with amplitudes of  $\sim 0.4$  mag. During the rising stage of the superoutburst (BJD 2458085), superhumps were barely observed. We performed the phase dispersion minimization method (PDM, Stellingwerf 1978) for the residual light curve between BJD 2457080–85. The 1 sigma errors for the PDM analysis were calculated by the method developed by Fernie (1989) and Kato et al. (2010). Figure 2 illustrates the resultant theta diagram, in which the strongest periodicity corresponds to  $P = 0.061181(42)$  d. This period is 4.0 % longer than the orbital period of QZ Vir, which safely excludes the orbital origin. Figure 3 shows phase-averaged light curves folded by  $P = 0.061181$

d, in which single-peaked profiles are visible. Such a single-peaked hump was also observed in an SU UMa-type dwarf nova PM J03338+3320 in the faint stage between the precursor and the main superoutburst (Kato et al. 2016a). They identified the observed single-peaked humps as superhumps, based on the period analyses and the profile of the humps. In combination with the above period, the modulations of the single-peaked light curves, and the previous report by Kato et al. (2016a), we can reasonably conclude that the single-peaked modulations are indeed superhumps.

In order to examine the characteristics of the superhumps, we calibrated superhump maxima and the amplitudes of superhumps. In general, measuring superhump maxima provide diagnostics of the dynamics in the outbursting accretion disk (Kato et al. 2009). The detailed method of calibration is the same as that described in Kato et al. (2009). In table 2, we tabulate the maximum timings of the superhumps and  $O - C$  values, where we used the following linear regression,

$$BJD(max) = 2457080.5836 + 0.06020 \times E. \quad (1)$$

Figure 4 shows the  $O - C$  diagram and amplitudes of the superhumps. As can be seen in these figures, a “break” occurred around  $E \sim 180$  and  $E \sim 195$ . Although our photometry was absent near the brightness maximum, the break in the  $O - C$  diagram may also have occurred around  $E \sim 100$ . Based on the obtained  $O - C$  diagram, we divided light curves into three segments, BJD 2457089.45–91.87 ( $147 \leq E \leq 188$ ), BJD 2457092.17–93.13 ( $193 \leq E \leq 208$ ), and BJD 2457093.67–111.81 ( $E \geq 217$ )<sup>2</sup>. For each segment, we performed the PDM method and the results of the period analyses are shown in figure 5. The best estimated period during  $147 \leq E \leq 188$  was  $0.060490(34)$  d, which is in good agreement with that obtained in the previous superoutbursts (e.g.,  $P_{sh} = 0.060488$  d for the 2005 superoutburst,  $P_{sh} = 0.060481$  d for the 2007 superoutburst, see also table 2 of (Kato et al. 2009)). We derived  $P_{sh} = 0.059944(24)$  d during  $193 \leq E \leq 208$ . This value is again in good agreement with that obtained in the previous superoutbursts of stage C superhumps (Kato et al. 2009). After the end of the main plateau stage (after BJD 2457095), we derived  $P_{sh} = 0.060000(9)$  d, 2.0 % longer than the orbital period of QZ Vir. This indicates that superhumps were sustained after the end of the main superoutburst.

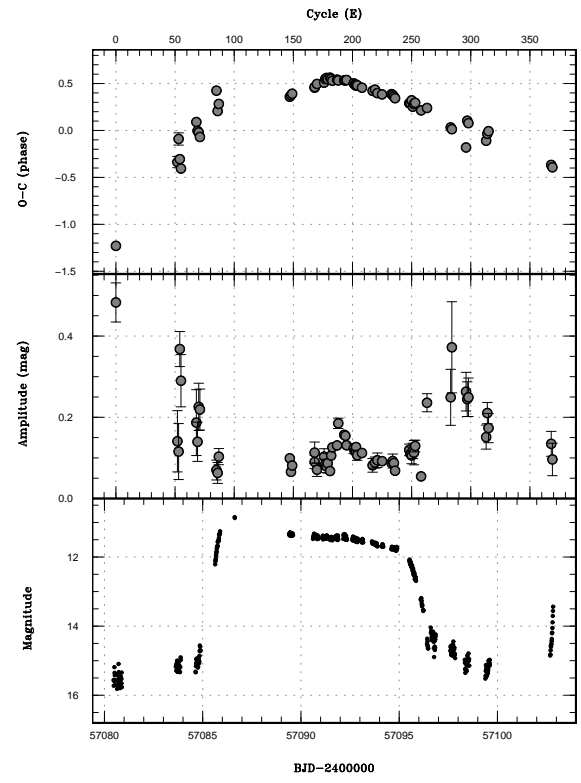


**Fig. 4.**  $O - C$  diagram of superhump maxima, amplitudes of superhumps, and corresponding light curve. A linear regression is expressed as equation 1. A ‘break’ is observed on BJD 2457092, when the stage B–C transition occurred. Stage A–B transition may have occurred between BJD 2457086–88, based on the PDM analyses for each segment (see figure 5).

## 4 Discussion

### 4.1 Stage A superhumps in the faint stage between the precursor and the main superoutburst

As noted above, one of the most important findings is that superhumps appeared after the end of the precursor and survived in the faint stage between the precursor and the main superoutburst. Kato et al. (2016a) recently reported that stage A superhumps were observed in the faint stage of a newly confirmed SU UMa-type dwarf nova PM J03338+3320 during the 2015 superoutburst. Kato et al. (2016a) noted that stage A superhumps first appeared near the end of the precursor and survived in the faint stage, after which the stage A–B transition occurred around the maximum brightness of the main superoutburst, based on their careful analyses of superhump period changes and amplitudes of superhumps. Although the individual maxima of superhumps were unable to be measured, stage A superhumps in the faint stage were also detected in the Kepler light curve of V1504 Cyg (Osaki, Kato 2014).

<sup>2</sup> Because of low quality of the data for period analyses, we did not use the data between BJD 2457119–22.

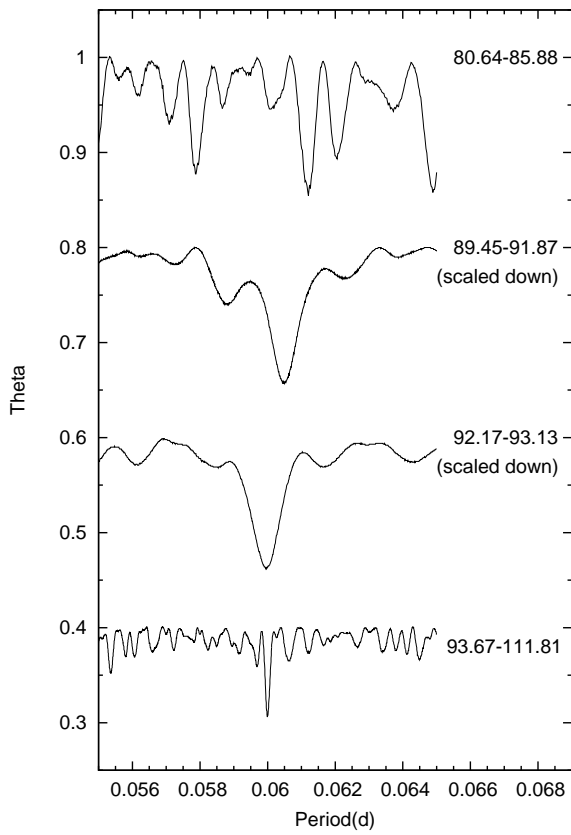


**Fig. 5.** Results of PDM analyses. The strongest periodicity corresponds to  $P = 0.060490(34)$  d for BJD 2457089.45–91.87,  $P = 0.059944(24)$  d for BJD 2457092.17–93.13, and  $P = 0.060000(9)$  d for BJD 2457093.67–111.81, respectively. For better visualization, the theta diagrams on BJD 2457089.45–91.87 and BJD 2457092.17–93.13 are scaled down arbitrarily.

In the case of QZ Vir, we detected a constant period of  $P_{\text{sh}} = 0.061181$  d in the faint stage. This period is 1.1% longer than that obtained between BJD 2457089.45–91.87. Kato et al. (2009) noted that the stage A superhump period is 1.0–1.5 % longer than the stage B superhump period in the same system. Although our observations were absent around the maximum brightness of the main superoutburst, the obtained  $O - C$  diagram in figure 4 indicates that a stage transition occurred around BJD 2457087 ( $E \sim 100$ ). The presence of stage transitions is also supported by the variations of the superhump amplitudes. Kato et al. (2009) reported that stage A superhumps have the largest amplitudes among three stages, and that a regrowth of superhump amplitudes is frequently seen in the stage B–C transition. In the middle panel of figure 4, the large amplitudes of superhumps are seen before BJD 2457087 ( $E < 100$ ), and a regrowth of the superhump amplitudes is observed around BJD 2457092 ( $E \sim 190$ ). In combination with the above results, we can reasonably conclude that the superhumps during the faint stage in QZ Vir are indeed the stage A superhumps.

Although the present observation is a rare case that stage A superhumps appear in the faint stage, the question remains how rare this phenomenon is. As noted above, there are only three SU UMa-type dwarf novae that exhibit stage A superhumps in the faint stage between the precursor and the main superoutburst: PM J03338+3320, V1504 Cyg, and QZ Vir. This rareness is due to insufficient data of the faint stage, or intrinsic rareness of this phenomenon. This should be clarified in future observations.

#### 4.2 Mass ratio and evolutional status of QZ Vir

As noted in the introduction, the mass ratio of QZ Vir is unclear, which obscures an evolutional status of the object. In recent years, Kato, Osaki (2013) have established a new method to estimate a mass ratio using the stage A superhump period. The method can extend to other systems including WZ Sge-type dwarf novae and AM CVn stars, if the stage A superhump period and the orbital period of the system are known (Isogai et al. 2016). Using a stage A superhump period during the 2014 superoutburst of QZ Vir, Kato et al. (2015) estimated a mass ratio to be 0.18(2). However, Kato et al. (2015) noted that this value should be improved in future observations, since the stage A superhump period was determined under a short coverage of observations.

In the present observations, sufficient data during stage A superhumps enables us to upgrade a mass ratio of QZ Vir. The obtained stage A superhump period and the known orbital period indicate a newly introduced excess/deficiency rate of  $\epsilon^* = 0.0386(7)$ , where  $\epsilon^*$  is written as  $\epsilon^* = 1 - P_{\text{orb}}/P_{\text{sh}}$ . Using table 1 of Kato, Osaki (2013), we obtain  $q = 0.108(3)$ . This value is very typical for SU UMa-type dwarf novae with short orbital periods, and significantly smaller than that derived by Shafter, Szkody (1984). The high mass ratio obtained by Shafter, Szkody (1984) ( $q \sim 0.48$ ) is possibly due to overestimation of the  $K_1$  value, which led to a light mass of the white dwarf ( $M_1 \sim 0.40 M_{\odot}$ ). The obtained mass ratio, orbital period and the absence of the secondary star in the optical spectrum exclude the possibility that QZ Vir contains an evolved secondary, like a possible progenitor for AM CVn stars (Podsiadlowski et al. 2003; Ishioka et al. 2007). This mass ratio also excludes the period bouncer of the system (Littlefair et al. 2006). The present result indicates that QZ Vir is an SU UMa-type dwarf nova evolving toward the period minimum.

#### 4.3 Time scale of stage A superhumps

Lubow (1991a) and Lubow (1991b) suggested that the

growth time of superhumps are inversely proportional to  $q^2$ . Observationally, it takes about a week for WZ Sge-type dwarf novae to exhibit superhumps (Kato 2015). Kato (2015) discussed a time scale of stage A superhumps, showing that systems with small mass ratios tend to have long time duration of stage A superhumps. This tendency is particularly seen in candidates for period bouncers (see figure 22 of Kato (2015)). In the case of the 2015 superoutburst of QZ Vir, the duration of stage A superhumps was about 5 d ( $\sim 80$  cycles), which is comparable to that of the candidates for period bouncers. As noted above, the mass ratio of QZ Vir obviously excludes the period bouncer of the system.

In order to explain such a long duration of stage A superhumps in the faint stage between the precursor and the main superoutburst of SU UMa-type dwarf novae, Kato et al. (2016a) suggest that a growth time of stage A superhumps needs a long time in a cold accretion disk. It is likely that the low viscosity state in the cold accretion disk requires more times to spread the eccentric mode into the entire disk (Kato et al. 2016a). The present observations further support this scenario. Based on the present and previous observations concerning the duration of stage A superhumps, it may be that the duration of stage A superhumps is mainly determined by two factors: mass ratio of the system and viscosity (or temperature) of the accretion disk.

## 5 Summary

We summarize the results of this paper as follows:

- We observed the 2015 February–March superoutburst of QZ Vir. The main superoutburst was separated from the precursor with the interval of  $\sim 5$  d. After the main superoutburst, QZ Vir showed a rebrightening.
- Superhumps were observed after the end of the precursor. During the faint stage between the precursor and main superoutburst, we estimated the superhump period to be 0.061181(42) d. This period was  $\sim 1.1\%$  longer than that observed in the previous superoutbursts. Based on the obtained  $O - C$  diagram of the superhump maxima, the long period of the superhumps, and variations of the superhump amplitudes, we identified the superhumps in the faint stage as stage A superhumps.
- Using the refined stage A superhump period, we determined a mass ratio of QZ Vir to be 0.108(3). In combination with the mass ratio and the optical spectrum of QZ Vir obtained by Shafter, Szkody (1984), we exclude the possibility that QZ Vir contains an evolved secondary star. This value also rules out the period bouncer of the

system. The present result indicates that QZ Vir is an SU UMa-type dwarf nova evolving toward the period minimum.

- It is likely that a cold accretion disk lengthens the duration of stage A superhumps. In combination with the present observations and the previous reports regarding the duration of stage A superhumps, a time scale of stage A superhumps is determined by the temperatures of the accretion disk and mass ratio of the system.

## Acknowledgments

We would like to thank the anonymous referee for helpful comments on the manuscript of the paper. This work was supported by the Grant-in-Aid Initiative for High-Dimensional Data-Driven Science through Deepening of Sparse Modeling E(25120007) from the Ministry of Education, Culture, Sports, Science and Technology (MEXT) of Japan. The authors are grateful to observers of VSNET Collaboration and VSOLJ observers. We acknowledge with thanks the variable star observations from the AAVSO International Database contributed by observers worldwide and used in this research.

## References

Cannizzo, J. K. 1993, in *Accretion Disks in Compact Stellar Systems*, ed. J. C. Wheeler (Singapore: World Scientific Publishing), p. 6

Cannizzo, J. K., Smale, A. P., Wood, M. A., Still, M. D., & Howell, S. B. 2012, *ApJ*, 747, 117

Cannizzo, J. K., Still, M. D., Howell, S. B., Wood, M. A., & Smale, A. P. 2010, *ApJ*, 725, 1393

Fernie, J. D. 1989, *PASP*, 101, 225

Hellier, C. 2001, *Cataclysmic Variable Stars: How and why they vary* (Berlin: Springer-Verlag)

Hirose, M., & Osaki, Y. 1990, *PASJ*, 42, 135

Ishioka, R., Sekiguchi, K., & Maehara, H. 2007, *PASJ*, 59, 929

Isogai, K., et al. 2016, *PASJ*, 68, 64

Kato, T. 1997, *PASJ*, 49, 583

Kato, T. 2015, *PASJ*, 67, 108

Kato, T., et al. 2016a, *PASJ*, 68, 49

Kato, T., et al. 2014a, *PASJ*, 66, 90

Kato, T., et al. 2015, *PASJ*, 67, 105

Kato, T., & Fujino, S. 1987, *Variable Star Bull.*, 3, 10

Kato, T., et al. 2013, *PASJ*, 65, 23

Kato, T., et al. 2014b, *PASJ*, 66, 30

Kato, T., et al. 2016b, *PASJ*, 68, 65

Kato, T., et al. 2009, *PASJ*, 61, S395

Kato, T., et al. 2012, *PASJ*, 64, 21

Kato, T., et al. 2010, *PASJ*, 62, 1525

Kato, T., et al. 2014c, *PASJ*, 66, L7

Kato, T., & Osaki, Y. 2013, *PASJ*, 65, 115

Lasota, J.-P. 2001, *New Astron. Rev.*, 45, 449

Lem, K., Patterson, J., Thomas, G., & Skillman, D. R. 1993, *PASP*, 105, 1120

Littlefair, S. P., Dhillon, V. S., Marsh, T. R., Gänsicke, B. T.,

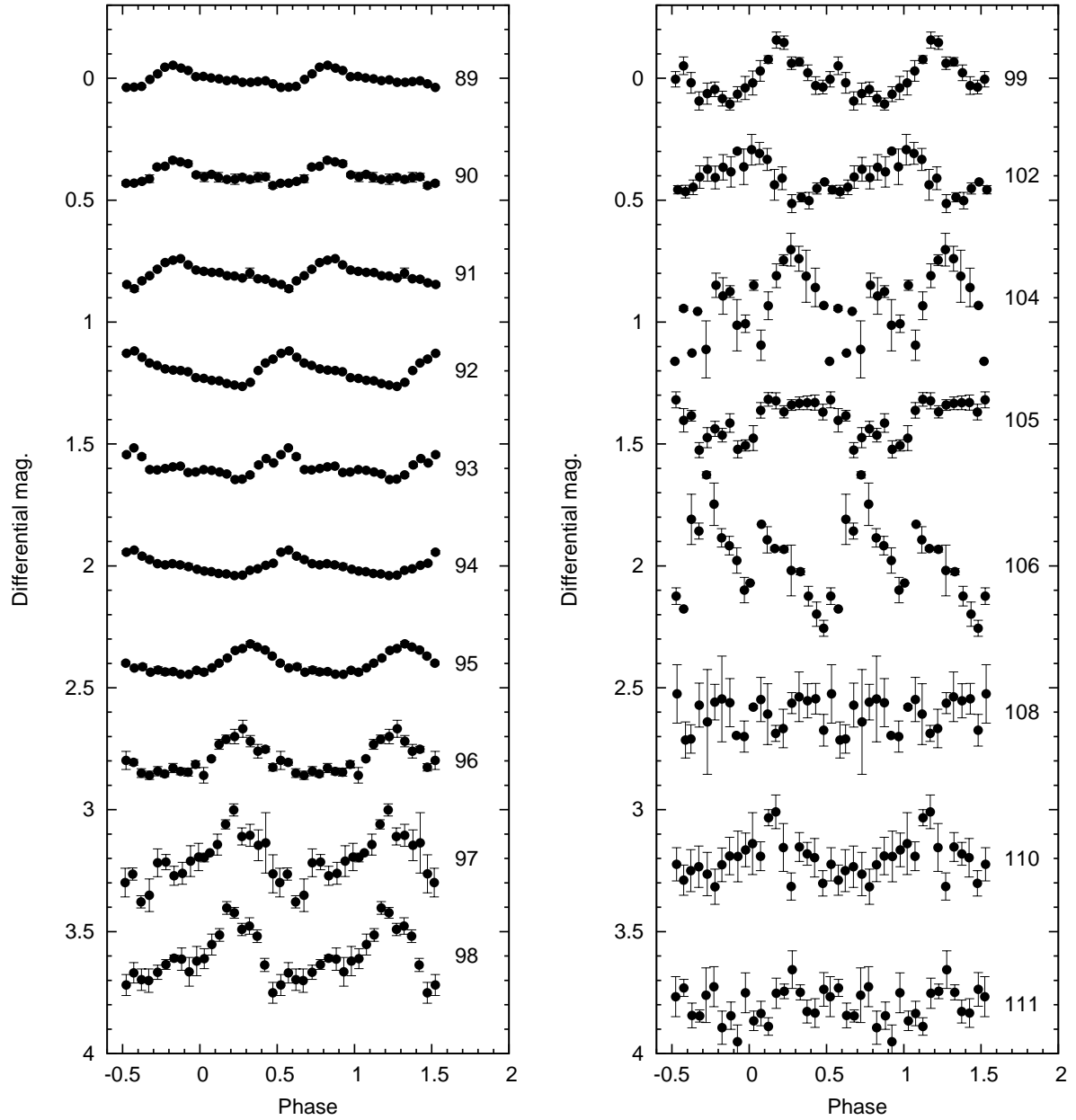


**Fig. 6.** Phase-averaged light curves between BJD 2457089–111. The numbers in this figure denote the day since BJD 2457000. The light curves are folded with 0.060490 d for BJD 2457089–91, 0.059944 d for BJD 2457092–93, and 0.060000 d for BJD 2457094–111, respectively.

Southworth, J., & Watson, C. A. 2006, *Science*, 314, 1578

Lubow, S. H. 1991a, *ApJ*, 381, 259

Lubow, S. H. 1991b, *ApJ*, 381, 268

Meyer, F., & Meyer-Hofmeister, E. 1981, *A&A*, 104, L10

Ohshima, T., et al. 2014, *PASJ*, 66, 67

Osaki, Y. 1974, *PASJ*, 26, 429

Osaki, Y. 1989, *PASJ*, 41, 1005

Osaki, Y. 1996, *PASP*, 108, 39

Osaki, Y., & Kato, T. 2013a, *PASJ*, 65, 50

Osaki, Y., & Kato, T. 2013b, *PASJ*, 65, 95

Osaki, Y., & Kato, T. 2014, *PASJ*, 66, 15

Otulakowska-Hypka, M., Olech, A., & Patterson, J. 2016, *MNRAS*, 460, 2526

Peters, C. H. F. 1865, *Astronomische Nachrichten*, 65, 55

Podsiadlowski, Ph., Han, Z., & Rappaport, S. 2003, *MNRAS*, 340, 1214

Schreiber, M. R., Hameury, J.-M., & Lasota, J.-P. 2004, *A&A*, 427, 621

Shafter, A. W., & Szkody, P. 1984, *ApJ*, 276, 305

Slovak, M. H., Nelson, M. J., & Shafter, A. W. 1987, *IAU Circ.*, 4314

Smak, J. I. 1991, *Acta Astron.*, 41, 269

Stellingwerf, R. F. 1978, *ApJ*, 224, 953

Vrielmann, S., Ness, J.-U., & Schmitt, J. H. M. M. 2004, *A&A*, 419, 673

Warner, B. 1995, *Cataclysmic Variable Stars* (Cambridge: Cambridge University Press)

Whitehurst, R. 1988, *MNRAS*, 232, 35

**Table 1.** Log of Observations.

Date	JD(start)*	JD(end)*	N†	Filter‡	Code§	Exp(sec)¶
2015 Feb. 26	7080.4585	7080.5539	108	V	RPc	60
2015 Feb. 27	7080.6397	7080.8782	100	C	HaC	180
2015 Mar. 2	7083.6313	7083.8784	106	C	HaC	180
2015 Mar. 3	7084.6288	7084.8809	104	C	HaC	180
2015 Mar. 4	7085.6266	7085.8801	107	C	HaC	180
	7086.4471	7086.4513	12	V	RPc	30
2015 Mar. 5	7086.6238	7086.6312	4	C	HaC	180
2015 Mar. 7	7089.3890	7089.5928	248	V	DPV	60
2015 Mar. 9	7090.6127	7090.8884	120	C	HaC	180
	7091.0860	7091.3328	226	R	Aka	90
	7091.1071	7091.2235	105	V	Aka	90
	7091.4317	7091.5975	214	V	DPV	60
2015 Mar. 10	7091.7487	7091.8891	118	C	HaC	180
	7092.1508	7092.3073	146	R	Aka	90
	7092.1670	7092.3321	157	V	Aka	90
2015 Mar. 11	7092.6076	7092.8901	193	C	HaC	180
	7093.0797	7093.1483	65	R	Aka	90
	7093.1042	7093.1497	44	V	Aka	90
	7093.1327	7093.1624	79	C	Kis	30
2015 Mar. 12	7093.6048	7093.8893	70	C	HaC	180
	7094.1099	7094.1753	62	R	Aka	90
	7094.1173	7094.1797	58	V	Aka	90
2015 Mar. 13	7094.6021	7094.8886	114	C	HaC	180
2015 Mar. 14	7095.5086	7095.6399	51	C	COO	120
	7095.5999	7095.8495	90	C	HaC	180
	7096.0878	7096.2277	162	C	Ioh	40
	7096.4042	7096.4723	89	C	Kai	60
2015 Mar. 15	7096.6036	7096.8457	66	C	HaC	180
2015 Mar. 16	7097.5943	7097.8427	77	C	HaC	180
	7098.3317	7098.5606	154	C	DPV	120
2015 Mar. 17	7099.3796	7099.6137	156	C	DPV	120
2015 Mar. 21	7102.6837	7102.8313	50	C	HaC	180
2015 Mar. 23	7104.7315	7104.8258	44	C	HaC	180
	7105.2813	7105.5438	177	C	DPV	120
	7105.3643	7105.5131	204	C	Kai	60
2015 Mar. 24	7106.3786	7106.4538	45	C	DPV	120
2015 Mar. 27	7108.5895	7108.8136	73	C	HaC	180
2015 Mar. 28	7109.5772	7109.8068	116	C	HaC	180
2015 Mar. 29	7110.5679	7110.8093	120	C	HaC	180
2015 Mar. 30	7111.5696	7111.8066	108	C	HaC	180
2015 Apr. 6	7119.3805	7119.5501	216	C	RPc	60
2015 Apr. 7	7120.3883	7120.4845	59	C	RPc	120
2015 Apr. 9	7122.3924	7122.4653	72	C	RPc	60

\* JD-2450000. † Numbers of images.

‡ The filter name C represents unfiltered observations.

§ Code of observers: RPc (R. Pickard, 34cm), HaC (J. Hambisch, 40cm), DPV (P. Dubovsky, 28cm)

Aka (H. Akazawa, 28cm for V filter, 20cm for R filter), Kis (S. Kiyota, 25cm)

COO (L. Cook, 32cm), Ioh (H. Itoh, 30cm), Kai (K. Kasai, 28cm).

¶ Exposure time in unit of seconds.

**Table 2.** Times of superhump maxima.

$E^*$	maximum time <sup>†</sup>	error <sup>‡</sup>	$O - C^§$	$N^{  }$
0	7080.50961	0.00064	-0.07400	52
52	7083.69374	0.00362	-0.02028	16
53	7083.76876	0.00393	-0.00545	21
54	7083.81603	0.00073	-0.01838	24
55	7083.87019	0.00116	-0.02443	17
68	7084.68263	0.00284	0.00542	12
69	7084.73715	0.00228	-0.00026	22
70	7084.79637	0.00148	-0.00124	23
71	7084.85364	0.00133	-0.00417	23
85	7085.72615	0.00214	0.02554	22
86	7085.77326	0.00242	0.01245	22
87	7085.83802	0.00120	0.01701	22
147	7089.45464	0.00040	0.02162	54
148	7089.51574	0.00052	0.02252	58
149	7089.57698	0.00043	0.02357	59
168	7090.72464	0.00114	0.02743	23
168	7090.66485	0.00146	0.02784	14
170	7090.78725	0.00136	0.02984	23
176	7091.14929	0.00105	0.03067	87
177	7091.21183	0.00085	0.03302	84
178	7091.27271	0.00118	0.03369	45
179	7091.33209	0.00153	0.03288	26
181	7091.45349	0.00058	0.03387	57
182	7091.51290	0.00037	0.03309	62
183	7091.57191	0.00027	0.03189	62
187	7091.81342	0.00031	0.03261	41
188	7091.87310	0.00039	0.03209	37
193	7092.17421	0.00028	0.03220	68
194	7092.23426	0.00026	0.03205	89
195	7092.29478	0.00035	0.03236	84
201	7092.65381	0.00058	0.03020	18
202	7092.71323	0.00040	0.02942	33
203	7092.83293	0.00050	0.02872	39
203	7092.77338	0.00035	0.02936	38
204	7092.89335	0.00079	0.02894	21
208	7093.13265	0.00036	0.02743	136
217	7093.67244	0.00227	0.02542	9
219	7093.79362	0.00091	0.02620	15
221	7093.85156	0.00106	0.02395	15
225	7094.15175	0.00036	0.02314	90
233	7094.63351	0.00072	0.02329	20
234	7094.69314	0.00094	0.02273	17
235	7094.75238	0.00075	0.02176	20
236	7094.81149	0.00084	0.02068	19
248	7095.53070	0.00068	0.01748	18
249	7095.59071	0.00062	0.01729	26
250	7095.65293	0.00128	0.01932	16
251	7095.70905	0.00101	0.01523	18
252	7095.77096	0.00150	0.01695	18

**Table 2.** (Continued)

253	7095.83194	0.00068	0.01773	19
258	7096.12809	0.00079	0.01288	80
263	7096.43063	0.00049	0.014413	51
283	7097.62215	0.00166	0.00193	15
284	7097.68121	0.00148	0.00079	14
296	7098.39190	0.00099	-0.01091	33
297	7098.46929	0.00096	0.00627	30
298	7098.52789	0.00113	0.00468	33
313	7099.41961	0.00123	-0.00660	33
314	7099.48429	0.00081	-0.00212	29
315	7099.54617	0.00127	-0.00045	33
368	7102.71511	0.00139	-0.02211	16
369	7102.77378	0.00220	-0.02364	16

\* Cycle count. † BJD-2450000.

‡ errors in units of days. § against equation 1.

|| Number of datapoints to determine the maximum time.